JOURNAL OF Applied Polymer SCIENCE

Electrically conductive polymeric bi-component fibers containing a high load of low-structured carbon black

Erik Nilsson,[1,2] Mikael Rigdahl,[2] Bengt Hagström[1,2]

[1]Materials Department, Swerea IVF, Box 104, SE-431 22 Mölndal, Sweden

[2]Department of Materials and Manufacturing Technology, Chalmers University of Technology, SE-412 96 Göteborg, Sweden

Correspondence to: E. Nilsson (E-mail: erik.nilsson@swerea.se)

ABSTRACT: Melt spinning at semi-industrial conditions of carbon black (CB) containing textiles fibers with enhanced electrical conductivity suitable for heating applications is described. A conductive compound of CB and high density polyethylene (HDPE) was incorporated into the core of bi-component fibers which had a sheath of polyamide 6 (PA6). The rheological and fiber-forming properties of a low-structured and a high-structured CB/HDPE composite were compared in terms of their conductivity. The low-structured CB gave the best trade-off between processability and final conductivity. This was discussed in terms of the strength of the resulting percolated network of carbon particles and its effect on the spin line stability during melt spinning. The conductivity was found to be further enhanced with maintained mechanical properties by an in line thermal annealing of the fibers at temperatures in the vicinity of the melting point of HDPE. By an adequate choice of CB and annealing conditions a conductivity of 1.5 S/cm of the core material was obtained. The usefulness of the fibers for heating applications was demonstrated by means of a woven fabric containing the conductive fibers in the warp direction. By applying a voltage of 48 V the surface temperature of the fabric rose from 20 to 30°C. © 2015 Wiley Periodicals, Inc. J. Appl. Polym. Sci. **2015**, *132*, 42255.

KEYWORDS: composites; conducting polymers; fibers; graphene and fullerenes; nanotubes

Received 2 October 2014; accepted 2 March 2015

DOI: 10.1002/app.42255

INTRODUCTION

Textile fibers have been utilized by mankind for centuries to protect the body from harsh environmental conditions.[1] For a long time fibers were collected from natural resources (e.g. cotton, flax, wool, silk) and the development was focused on wearing comfort, aesthetic aspects, and manufacturing technologies and was in fact an important driver for the industrialization during the 19th century. In recent times more and more efforts have been spent to impart various functionalities to textiles. An example of such functionality is electrical conductivity, which plays a crucial role in the emerging field of smart textiles[2] and is utilized in applications like anti-static protection, electromagnetic interferences (EMI) shielding, sensors, signal transfer and heating. To achieve a very high conductivity of the yarn, from which textile fabrics are woven or knitted, thin metal wires can be combined with textile fibers in various ways.[2] Another approach is to coat the fibers with a thin metal layer.[3] However, there are certain drawbacks in using metals, associated e.g. with degradation by wear and tear and durability during textile manufacturing or use.[4] Furthermore, corrosion and oxidation can occur, leading to failure due to lack of conductivity.

Thus, there are good arguments for seeking other ways of making textile fibers conductive. Our research group has recently investigated the possibility of using conductive polymer composites in the manufacturing of melt-spun textile fibers.[5–8] Conductive carbon nanoparticles, carbon black (CB), carbon nanotubes (CNT) and, recently, graphite nanoplatelets (GNP), have gained intense attention during the last decades. The addition of an adequate amount of such particles to the polymer dramatically improves its properties and adds functionality to the polymer.[9–11] The ability of a conductive polymer composite (CPC) to be processed into a fiber depends on several factors, e.g. compounding history, polymer matrix, processing conditions and the specific filler used. When GNPs are used as filler, fibers with high loadings can be produced, but the uniaxial elongational flow during spinning orients the platelets in the direction of flow and the conductivity is significantly impaired.[8] With CNTs in a fiber, the cylindrical CNTs will be oriented in the axial direction of the fiber.[12] Consequently, the conductivity of the fibers is reduced with increasing draw-down ratio.[6,13,14] Thus CB, although its lower inherent conductivity compared to CNT and GNP, would be the most favourable option for melt spinning applications since it is less affected by flow orientation

effects. Furthermore, the decrease in conductivity of a polymer/CB composite during the drawing can be restored by heat treatment, which is not the case for polymer/CNT or polymer/GNP composites.[7,8]

However, the addition of CB (as also CNT and GNP) to a thermoplastic polymer has its drawbacks related to processability. As a result of the formation of a percolated network of carbon particles, a strong viscosity enhancement and pronounced melt elasticity, accompanied with a yield stress phenomenon follow. This has a negative effect on the fiber spinning in terms of spin line instabilities, fiber diameter variations and ultimately, as the melt draw ratio increases, spin line breakage.[15] To overcome some of these difficulties it was recently proposed to use bi-component technology,[7] where the fibers have a conductive composite in the core surrounded by a fiber forming polymer in the sheath. The main part of the spin line stress is then taken up by the sheath polymer relieving some of the requirements on spinnability of the CPC core material. Bi-component fibers with a PA6 sheath and a core material of CB filled HDPE with a conductivity of 0.35 S/cm in the core were then produced.[7]

It has been shown that different types of CB give different types of electrical percolation behaviour. A more branched structure has a lower percolation threshold.[16,17] The melt rheological properties of the composite also depends on the structure of CB used, cf.,[18] which is also reflected in the processing properties.[19,20] However, little or no attention has been given to how the CB structure influences the properties of melt-spun fibers. The objective of present study is evaluate how a low structured CB composite (in comparison to a high structured CB) influence the spinning process and fibers final electrical conductivity. Also, there is a need to further enhance the conductivity of the fibers, especially for heating applications. Thus, there are good motives for assessing the effect of CB type on spinnability and resulting conductivity, which is the aim of the present study. More specifically, the focus is on the feasibility of melt spinning a conductive HDPE/CB composite incorporated as the core in bi-component fibers. The influence of in-line heat treatment of bi-component fibres is also evaluated.

EXPERIMENTAL

Materials

The polymer used for preparation of the core compound was a high density polyethylene (HDPE) ASPUN 6835A from Dow (Midland, MI); MFI (melt flow index) = 17 g/10 min at 190°C (for 2.16 kg), density = 950 kg/m^3 and melting point 129°C. The polymer for the sheath was polyamide 6 (PA6), Ultramide B33L obtained from BASF, Germany with a density of 1130 kg/m^3. The low surface area carbon black (LS-CB) grade was Ensaco 250 from Timcal, Switzerland with a density of 1900 kg/m^3, a bulk density of 185 kg/m^3 a BET surface area of 65 m^2/g and an Oil Absorption Number (OAN) of 190 mL/100 g. The high surface area grade CB (HS-CB) was Ketjenblack 600 JD from Akzo Nobel, the Netherlands, with a density of 1800 kg/m^3, a bulk density of 100–120 kg/m^3, a pore volume (DBP) of 480–510 mL/100g and a BET surface area of 1400 m^2/g. All data as given by the suppliers.

Composite Manufacturing

The core composite was compounded using a Coperion (ZSK 26 K 10,6, Germany) co-rotational twin screw extruder with 10 heating zones. The barrel temperature profile was set to: zone 1: 165°C and zones 2-10: 205°C, starting from the hopper inlet. The screw speed was 230 rpm. The final filler content was controlled by adjusting the feeding rate of the polymer and CB, the total throughput being set to 10 kg/h. The extrudate was solidified in a water bath and pelletized using a strand cutter.

Production of Strands for Conductivity Measurements and Monofilament Spinning

Fiber spinning and production of undrawn strands was performed using a capillary rheometer (CEAST Rheoscope 1000 manufactured by CEAST Turin, Italy). Undrawn strands were produced with a 10-mm long capillary with a diameter of 1 mm. For melt drawing trials a different die was used: the leading and middle portion diameter was 9.50 mm and 2.50 mm, respectively, with 45° cone angle. The exit capillary length was 1.2 mm with diameter (d_{cap}) 0.6 mm. The diameter of the barrel (d_{bar}) was 9.55 mm and piston speed (V_p) 20 mm/min. The exit velocity of the melt (V_0) was calculated according to eq. (1). During spinning, the speed of the take-up wheel was gradually increased until spin line breakage occurred (at V_b) and the critical melt draw ratio (MDR@break) at break was then calculated using eq. (2). The exit velocity at the die was 5.1 mm/min, which corresponds to an apparent shear rate at the capillary wall of 1120 s^{-1}. For composites with a low spinnability, a set-up with a guide wheel was used as shown in Figure 1. The distance from the capillary die to the wheel was 0.85 m and between the wheel and the winder it was 1.75 m. For production of the undrawn strands a piston speed of 5 mm/min was used and strands with a length of about 15 cm were collected with a pair of tweezers. The temperature was set to 230°C in all experiments.

$$V_0 = V_p \frac{{d_{bar}}^2}{{d_{cap}}^2} \quad (1)$$

$$MDR_{@break} = \frac{V_b}{V_0} \quad (2)$$

Morphology Characterization

Cross-sections of strands and fibers were ion polished (Gatan model 693, USA) to obtain a smooth surface for the scanning electron microscopy (SEM) analysis. Micrographs were obtained using a field-emission gun SEM (FEG-SEM) JSM 7800 F from Jeol, Japan.

Rheological Measurements

Dynamic rheological measurements were performed at 230°C using a cone and plate rheometer (CS melt, Bohlin, Sweden). The cone diameter was 15 mm and the cone angle 5.4° and the measurements were performed under nitrogen atmosphere. The shear amplitude used was 0.1–1% depending on the filler content and was within the linear viscoelastic region. The same instrument and temperature was used for determining the shear stress (shear strain) relation. A Rheograph 2002 capillary viscometer (Göttfert, Germany) was used to measure the apparent shear viscosity. The capillary had a length of 10 mm, a diameter

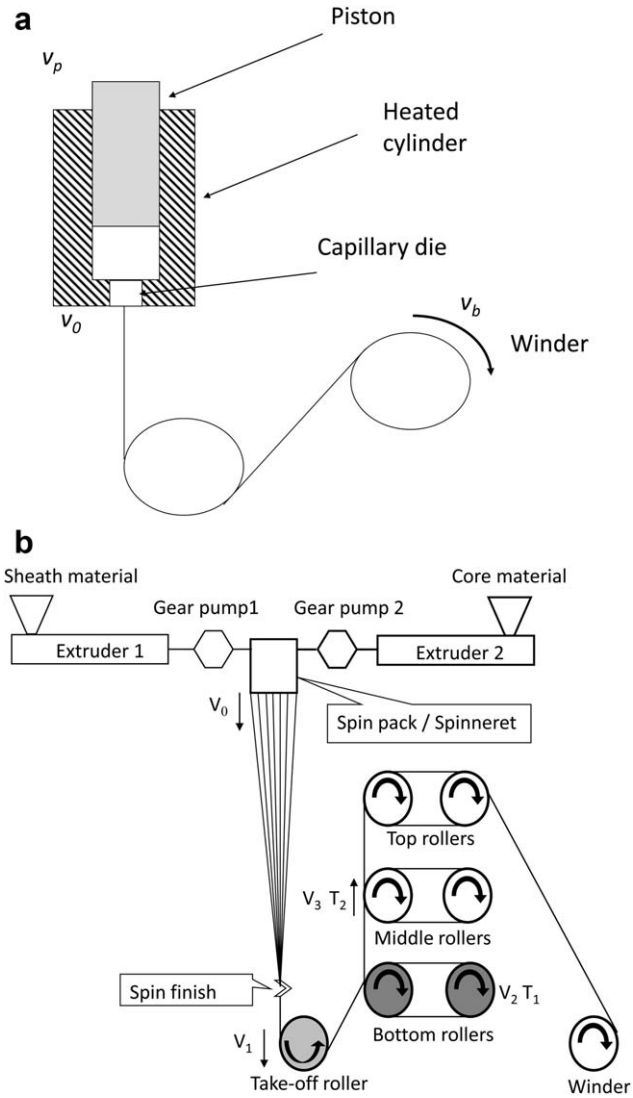

Figure 1. To the left, picture of equipment used for determining the MDR at break and to the right, schematic drawing of the melt spinning equipment used for production of bi-component fibers.

of 1 mm and an entrance angle of 180°. The pressure was measured with a transducer with a pressure range of 0–500 bar. The temperature was 230°C and the shear rate range was 30–3000 L/s.

Bi-Component Fiber Manufacturing

Bi-component fiber spinning was performed using a melt spinning line from Extrusion Systems Limited (ESL, Leeds, England), schematically shown in Figure 1. Fibers were spun at different combinations of the melt draw ratio (MDR = V_1/V_0), the solid state draw ratio (SSDR = V_3/V_2) and the godet roll temperatures (T_1 and T_2). The velocities V_0, V_1, and V_3 as well as the roll temperatures are explained in Figure 1. The diameter of the fibers produced was controlled by the total draw ratio (*MDRxSSDR*) through the entire system. The temperature settings were as follows: Extruder 1 (sheath) zones 1, 2 and 3: 220°C, 270°C, and 270°C, respectively; Extruder 2 (core) zones 1, 2 and 3: 210°C, 270°C, and 270°C, respectively. The temperature of the spinneret and the metering pumps was set to 270°C. Table I shows the spinning parameters for the fibers produced.

Measurement of the Electrical Conductivity

The conductivity measurements were performed using the two-probe method on un-drawn 100 mm long strands with a diameter of 1 mm. In case of the bi-component fibers, a bundle of fibers was cut with a razor blade and contacted with silver paint at the ends. The applied voltage, using a voltage supply (Oltronix D400-007D, Sweden), was varied between 10 and 50 V depending on the sample resistance. The current was measured with a digital multimeter (Fluke 8846A, USA). The volume conductivity σ_v was calculated as:

$$\sigma_v = \frac{\rho l^2 I}{mU} \tag{3}$$

where ρ is the density of the core material, l is the length of the fiber bundle, I is the measured current, m is the mass of the core material and U is the measured voltage. For each system, five specimens were measured.

The electrical conductivity of the fibers was also measured during heating and cooling in an oven. A set-up similar to the one described above was used, but with a different multimeter (Thurlby 1905a, England) connected to a computer continuously logging the current. The temperature was measured using a resistance thermometer, Pt100, placed in the vicinity of the fibers, and connected to a temperature logger (Kimo Kistock KTT310, France). The temperature was raised from ambient to 150°C at a rate of 4°C/min.

Tensile Testing of Fibers

The fiber titer and tenacity was determined on single filaments using a Vibroscope/Vibrodyn device (Lenzing, Austria). The distance between the clamps was 20 mm and the test speed 20 mm/min. The results given are averages of 24 tested samples.

Thermal Properties

Differential scanning calorimetry (DSC) analyses were performed using a TGA/DSC 1 (Metler Toledo, Switzerland). Scans were performed at a heating/cooling rate of 10°C/min. Specimens prepared from a pelletized sample of the CPC were placed in an aluminum pan. Each sample was heated well above the melting temperature and subsequently cold. The results shown are from the first heating scan. Measurements were made on three samples.

RESULTS AND DISCUSSION

Electrical Conductivity of the Core in the Bi-Component Fibers

Figure 2 shows the electrical conductivity versus the filler volume fraction of the LS-CB/HDPE composite. The coefficient of variation was less than 10% calculated using five samples at each filler loading. The curve in the graph represents a power law fit according to classic percolation theory:

$$\sigma = \kappa(v_f - v_c)^{\beta} \tag{4}$$

where σ is the conductivity of the composite, κ is regarded as a fitting parameter related to the conductivity of the filler, v_c is the percolation threshold, v_f the volume fraction of CB and β is

Table I. Spinning Parameters and Electrical Properties of the Produced Bi-Component Fibers

Sample no.	Vol % carbon i n core	Vol % core material	Die exit speed, V_0 (m/min)	Take off roller, V_1 (m/min)	Middle roller, V_2 (m/min)	MDR	SSDR	Temperature Bottom roller, T_1 (°C)	Temperature middle roller, T_2 (°C)	Conductivity (S/cm)
1	26	25	5.66	259	529	47	2	70	70	0.15
2	26	25	5.66	259	529	47	2	130	130	0.76
3	26	33	6.37	259	529	41	2	130	130	
4	26	38	4.60	211	430	47	2	50	50	0.31
5	26	38	4.60	211	430	47	2	70	70	0.44
6	26	38	4.60	211	430	47	2	80	80	0.72
7	26	38	4.60	211	430	47	2	90	90	1.19
8	26	38	4.60	211	430	47	2	100	100	1.17
9	26	38	4.60	211	430	47	2	120	120	1.06
10	26	38	4.60	211	430	47	2	130	130	1.39
11	26	38	4.60	211	430	47	2	140	140	1.27
12	26	38	4.60	211	430	47	2	70	140	0.72
13	26	38	4.60	211	430	47	2	130	140	
14	26	38	4.60	147	150	33	2	130	140	1.50
15	26	46	4.60	211	430	47	2	130	140	
16	22.1	25	5.66	488	996	88	2	70	70	0.19
17	22.1	33	6.37	488	996	78	2	70	70	
18	18.4	25	5.66	558	571	101	1	70	70	0.47
19	18.4	25	5.66	279	569	50	2	70	70	0.18
20	18.4	25	5.66	186	569	33	3	70	70	0.14
21	18.4	25	5.66	976	997	176	1	70	70	
22	18.4	25	5,66	488	996	88	2	70	70	
23	18.4	25	5.66	326	997	59	3	70	70	

the critical exponent related to the dimensionality of the conductive filler network. The parameters in the equation were obtained from the experimental data using a least squares linear regression. According to classic percolation theory, three dimensional systems of randomly distributed spherical particles typically have a critical exponent between 1.5 and 2.0.[21] The present system had a critical exponent β of 2.4, somewhat larger than the stated range. In our previous studies using a CB with a substantially higher surface area, a similar value of β (2.3) was found,[6] but a value as high as 2.9 was recently reported for CB/HDPE systems.[22]

As shown in Figure 2, the percolation threshold was achieved at 4.1 vol % filler for the LS-CB composite. With the same HDPE grade as polymer matrix, but using HS-CB with a higher surface area the threshold was 1.0 vol % filler.[6] Figure 3 shows SEM micrographs of the two composites at the same volume concentration (5.3 vol %). The large difference in morphology and electrical conductivity between the two composite systems is likely to be attributed to the difference in specific surface area and structure between the two CB grades, cf.[19] In Ref. 23 micrographs of injection-molded samples, where the polymer on the surface was removed by etching, revealed that primary aggregates in a high-structured CB formed a well-defined network in contrast to that of a low-structured CB forming of what appears to be somewhat larger aggregates with only a few contact points. The HS-CB has both a larger surface area and smaller primary particles which is known to contribute to the highly branched aggregate structure (or morphology) present in the HS-CB grade[24] thus reducing the percolation threshold compared to the LS-CB. Figure 3 certainly indicates that the high structured CB forms a dense network and thus gives a lower percolation threshold and a higher conductivity at given filler loading in the vicinity of percolation threshold. The electrical conductivity of the 5.3 vol % HS-CB composite was 0.2 S/cm compared to 0.002 S/cm for the LS-CB material.

Rheological Properties and Spinnability of the Core Composite

Figure 4(a) shows the storage modulus G' of unfilled HDPE and of its nano-composite with different loadings up to 26 vol % of LS-CB as a function of the angular frequency at 230°C. Not surprisingly the storage modulus increased as the filler content increased. At higher amounts of CB, the frequency dependence of the modulus became less pronounced indicating a plateau at low frequencies. Such a plateau indicates the formation of a percolated particle network. The material containing the HS-CB had storage modulus in the low frequency range that was almost three orders of magnitude greater than that of the LS-CB at the same filler volume fraction of CB (5.3 vol %). The HS-CB thus develops a much stronger network than the LS-CB that will have repercussions on the melt spinnability.

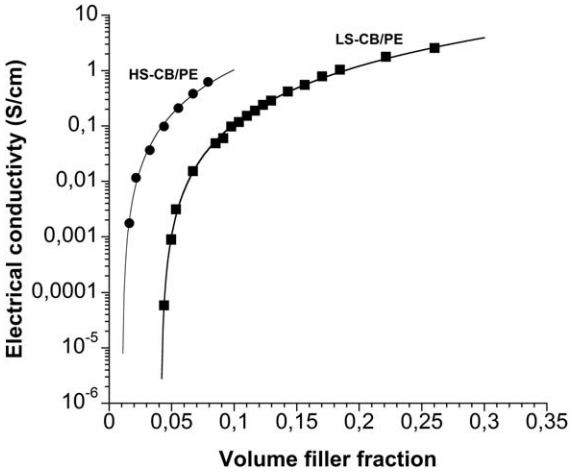

Figure 2. Electrical percolation behaviour of LS-CB in PE compared with data for HS-CB in PE from Ref. 7.

Figure 4(b) shows the magnitude of complex viscosity $|\eta^*|$ versus angular frequency ω and the steady state shear viscosity versus shear rate for the same materials as in Figure 4(a) and also for PA6. For filled polymer systems, the slope of the viscosity versus frequency curve at higher filler contents approaches -1 in this double logarithmic plot at lower frequencies indicating a yield stress, i.e. a transition from liquid like to solid-like behavior.[6] At higher shear rates (obtained with the capillary viscometer) which are more relevant to the shear rates at hand in the melt spinning process,[25] PA6 (used in the sheath) had a viscosity not far from that of the core composite materials. Evidently the Cox-Merz rule fails for the particle filled polymers, cf.[26] From Figure 4(a,b) it is evident that HS-CB clearly had a greater impact on the rheological response than LS-CB. A similar observation was recently made by Ren *et al.*[20] and they concluded that the HS-CB network was more stable at large strains compared to LS-CB and that LS-CB aggregates had stronger tendency for and re-aggregation in the polymer melt.

Figure 5 shows both the shear yield stress $Y_s(\varphi)$ and plateau storage modulus $G'(\varphi)$ for the LS-CB/HDPE composites as a function of filler volume fraction at 230°C. Rheological shear stress measurements were performed in a controlled stress mode and plateau modulus is the storage modulus at the lowest frequency from Figure 4(b). The yield stress was detected by gradually increasing the torque (shear stress) applied to the cone in the rheometer until meaningful readouts were noted. The very low shear rate values in Figure 6 are fictitious since they

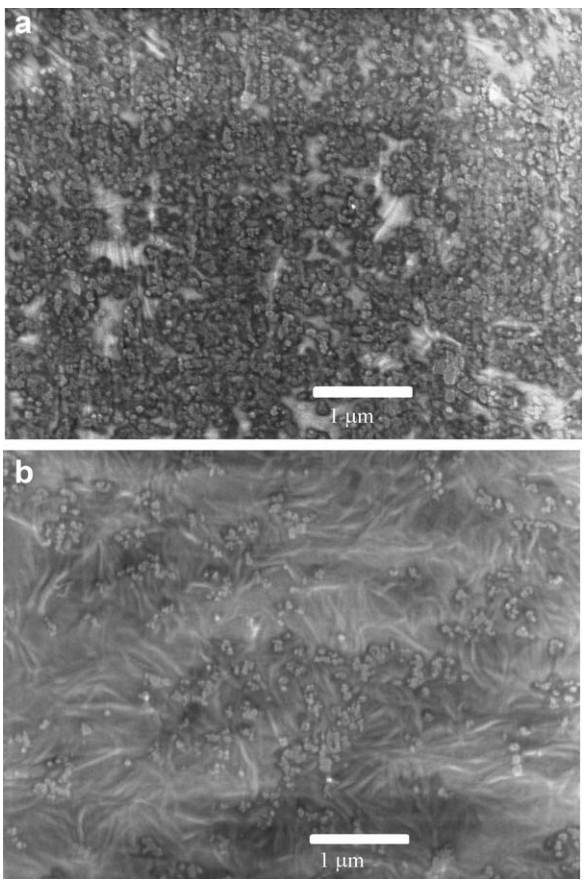

Figure 3. Micrographs of ion polished cross sections of extruded strands with 5.3 vol % CB in HDPE. a) HS-CB and b) LS-CB.

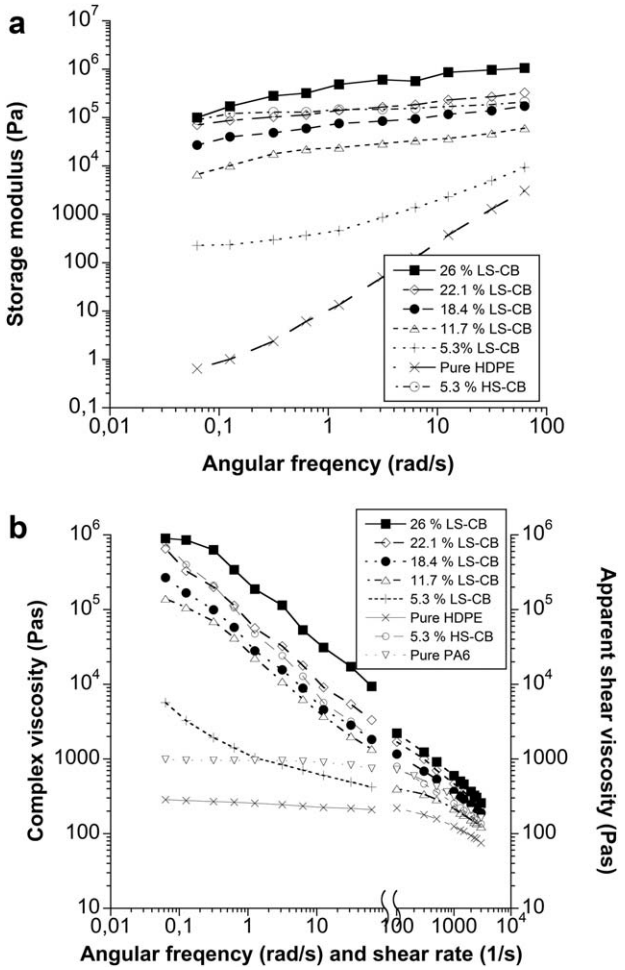

Figure 4. (a) Storage modulus of CB/PE composites at different filler volume concentrations as function of angular frequency. (b) Complex viscosity and apparent shear viscosity of the polymers and their blends with CB as function of angular frequency and apparent shear rate.

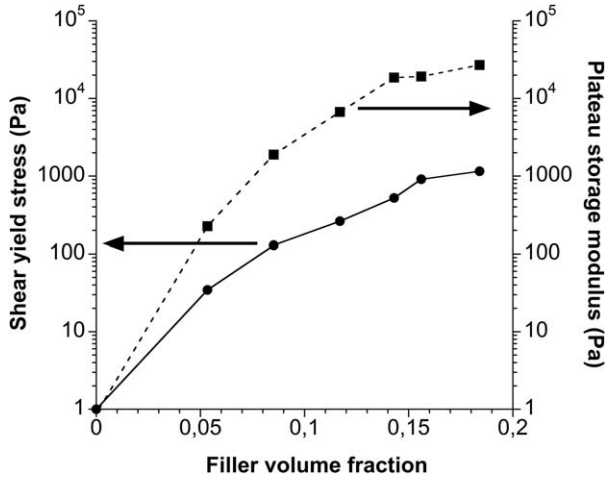

Figure 5. Shear yield stress and storage modulus plotted versus filler volume fraction for LS-CB/HDPE composites used for fiber production.

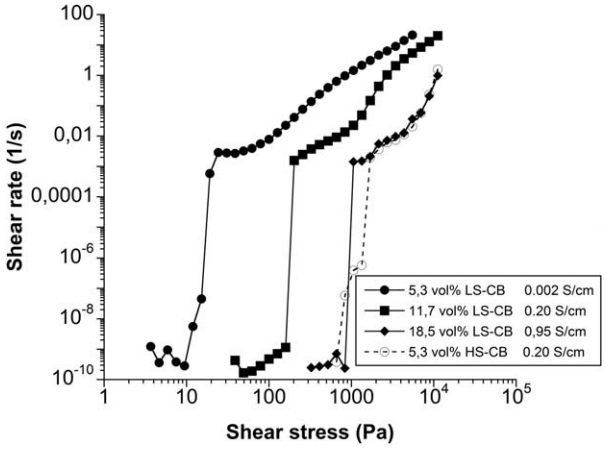

Figure 6. Shear rate as a function of shear stress for LS-CB at different filler contents and 5.3 vol % HS-CB in the PE matrix.

represent shear rates calculated by the rheometer software from the magnitude of the electrical noise of the rotation angle meter while the cone actually is at rest. Both $G'(\varphi)$ and $Y_s(\varphi)$ exhibit a power law type of relation to the filler volume fraction. The ratio of $G'(\varphi)$ to $Y_s(\varphi)$ is roughly about 0.1 as seen in Figure 5. Based on Hooke's this indicates that that yielding (breaking the intrinsic carbon particle network) occurs at a shear strain of about 10%. Figure 6 reveals that the HS-CB containing HDPE exhibited a higher Y_S value than LS-CB at a given volume concentration. The yield stress of the HS-CB composite was approximately two orders of magnitude greater than that of the LS-CB composite at the same filler volume fraction. HS-CB obviously formed a stronger intrinsic network at a given filler concentration and filler–filler interactions normally have a larger impact on the rheological behavior than filler–polymer interactions.

Spinnability. Figure 7 shows the maximum attainable melt draw ratios vs the filler content from the spinning experiments using the capillary rheometer. Up to 9% CB the spin line was intact even at the highest attainable winding speed corresponding to a MDR of 207. At higher filler concentrations, the melt draw ratio at break gradually decreased with increasing filler concentration. At 15% CB and above, spin line instabilities were visually observed and MDR@break exhibited a large scatter. For filled polymer systems, it has been shown that materials with a high yield stress exhibits poor spinnability.[27] During melt spinning, as the take-up speed increases, the spin line extensional rate increases and thus also the extensional stress in the melt. In melt spinning of filled polymer systems, the extensional yield stress is of great importance,[28] but is difficult to measure. Tanaka and White[29] indicated however a relation between the shear and elongational properties of filled polymer melts which supports the correlation between the shear yield stress and the spinnability noted here.

When manufacturing electrically conductive fibers the two important factors to consider are the spinnability and the conductivity. The results obtained shows that the LS-CB and HS-CB composites can exhibit a similar rheological response but differ in electrical conductivity by almost one order of magnitude. For example, the 5.3 vol % HS-CB/HDPE composite had a Y_s-value similar to that of the 18.4 vol % LS-CB composite, but the electrical conductivity of the HS-CB composite was 0.2 S/cm compared to 0.95 S/cm for the LS-CB. The LS-CB could barely be spun to a fiber with a MDR of 10, whereas the HS-CB was not spinnable at all. However, as seen in Figure 7 LS-CB composite (11.7 vol % CB) with a conductivity of 0.2 S/cm could almost be spun with a *MDR* of 100. The disturbance of the spin line could be caused by structural differences of the filler, the HS-CB having a more branched structure and thus a larger hydrodynamic volume than the LS-CB. When the hydrodynamic volume of the aggregates overlaps, preventing the free rotation of the agglomerates, the shaping of the melt into a fiber is hindered. It has been shown that a high-structured CB composite melt could withstand a larger strain than a low-structured CB[20] indicating a stronger rheological network. This could be a possible explanation why the HS-CB composite could not be spun. Based on these findings it seems reasonable to assume that the LS-CB would represent a better trade-off between conductivity and processability.

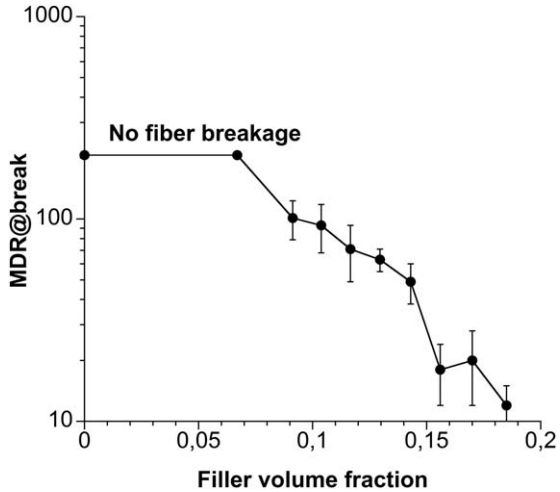

Figure 7. Maximum attained melt draw ratio at break plotted versus filler volume fraction of LS-CB/HDPE composites.

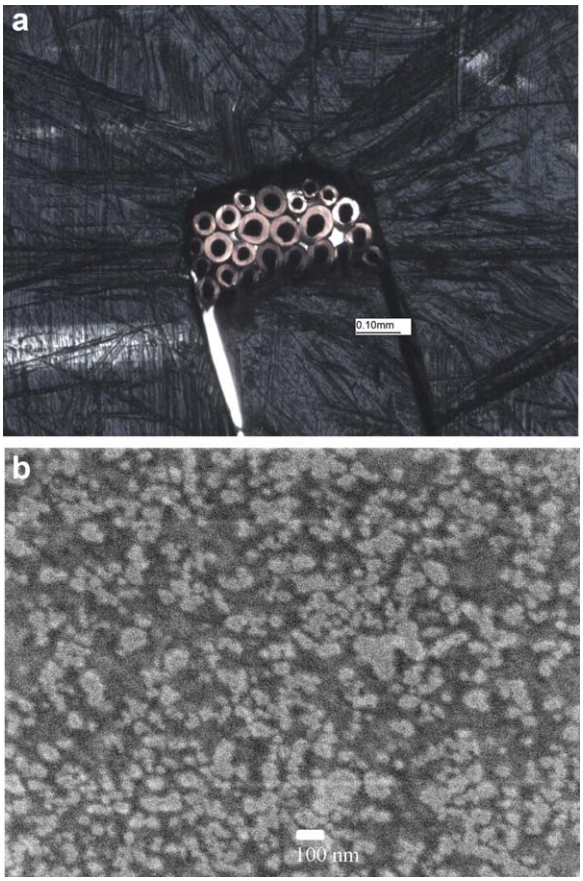

Figure 8. (a) Bi-component fibers with a conductive composite containing 26 vol % LS-CB, (a) a bundle of fibers and (b) the carbon filler network in the core appearing more whitish than the darker polymer matrix. [Color figure can be viewed in the online issue, which is available at wileyonlinelibrary.com.]

Melt Spinning of Bi-Component Fibers Using LS-CB in the Core Material

As noted above, an increased filler loading reduced the drawability of the composite and the resulting fiber was too brittle for further processing into a textile. Using sheath/core bi-component technology, i.e. surrounding the composite with a load-bearing sheath, can be a way to produce a fiber with sufficient strength.[7] Multifilament yarns with a high molecular weight PA6 sheath with different CB contents in the LS-CB/HDPE core were produced; these fibers contained 18, 22, and 26 vol % CB in the core material. The electrical properties are summarized in Table I. The attainable *MDR* and *SSDR* decreased as the CB content in the core composite increased, and the yarn titer thus had to be increased to obtain a coherent core. Fibers containing 18 vol % CB could be drawn with *SSDR* up to 3, and this was also the limit for fibers with unfilled HDPE in the core. The maximum *SSDR* of single component fibers of the PA6 grade used and produced under similar conditions was also about 3. Thus, neither the pure HDPE in the core, nor the 18 vol % CB composite, limited the attainable *SSDR*. To produce fibers containing 22 and 26 vol % CB, a reduction to 2 in *SSDR* was required for achieving a stable spin line without filament breakage. The high viscosity of the core material then required a higher die head pressure, up to the limit of the equipment. The sheath/core volume flow was balanced to obtain the maximum amount of core material in the fibers under steady process conditions. Optical and SEM micrographs of fiber cross-sections in Figure 8 show the conductive filler network appearing as the whitish structure in the right-hand image.

Influence of Cold Drawing and Annealing Temperature on the Electrical Properties of the Bi-Component Fibers

To obtain sufficient strength of a melt spun fiber, the fiber must be cold drawn. This involves stretching the fibers in the solid state, a process that has a negative influence on the conductivity of the fibers. The electrical volume conductivity of the fibers containing 18 vol % CB was reduced from 1 S/cm for the undrawn strand to 0.47 S/cm for fibers produced with MDR = 101, SSDR = 1, and to 0.15 S/cm for MDR = 33, SSDR = 3. Previous studies[7] have shown that SSDR had a stronger influence on the electrical properties of the fibers than MDR which is in line with the present findings.

By heat treating the fibers in an oven above the melting point of the fiber core, the conductivity can be restored.[7] Here the fibers were heat treated on the godet rolls during spinning. Table II shows how the temperature of the godet rolls influenced the conductivity of the fibers. The fibers could be heat treated either by heating both the bottom rolls and the middle rolls above the melting point of the core material or by just heating the middle rolls above the melting point. The heat treatment was however more efficient if both pairs of rolls were heated.

When the fibers were cold drawn (between bottom and middle rolls) at a temperature below the melting point of the core material but annealed above the melting point on the middle rollers, the rearrangement of the CB particles (restoring the conductivity) was surprisingly fast. The total residence time on the heated godet rolls was as short as 0.8 s and the conductivity increased from 0.44 S/cm to 0.72 S/cm. The effect of varying the temperature of the godet rolls is illustrated by samples 4–11 in Table I where T_1 and T_2 were varied between 50 and 140°C. The metering pump was set so that the maximum amount of core material could be incorporated into the fibers (sheath/core volume ratio = 8/5) still keeping the spinning process stable. The titer was 26 dtex/fiber, tenacity was 23.7 (±2.5) cN/tex, elongation at break 105.1 (±37.1) % and Young's modulus 126 (±36) cN/tex. Increasing the godet rolls temperature from 70°C to 140°C had a negligible influence on the mechanical properties (tenacity was 24.6 ± 2.8 cN/tex). Figure 9 shows the

Table II. Influence of Godet Roll Temperature on the Electrical Conductivity of Bi-Component Fibers with 26 vol % CB

Rollers	Temperature (°C)		
Bottom rollers, T_1	70	70	140
Middle rollers, T_2	70	140	140
Electrical conductivity (S/cm)	0.44	0.72	1.27

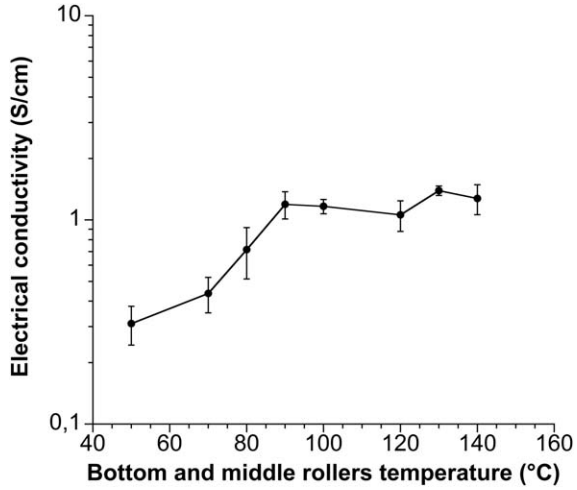

Figure 9. The electrical conductivity versus the temperature of the bottom and middle rolls for fibers containing 26 vol % CB in the core.

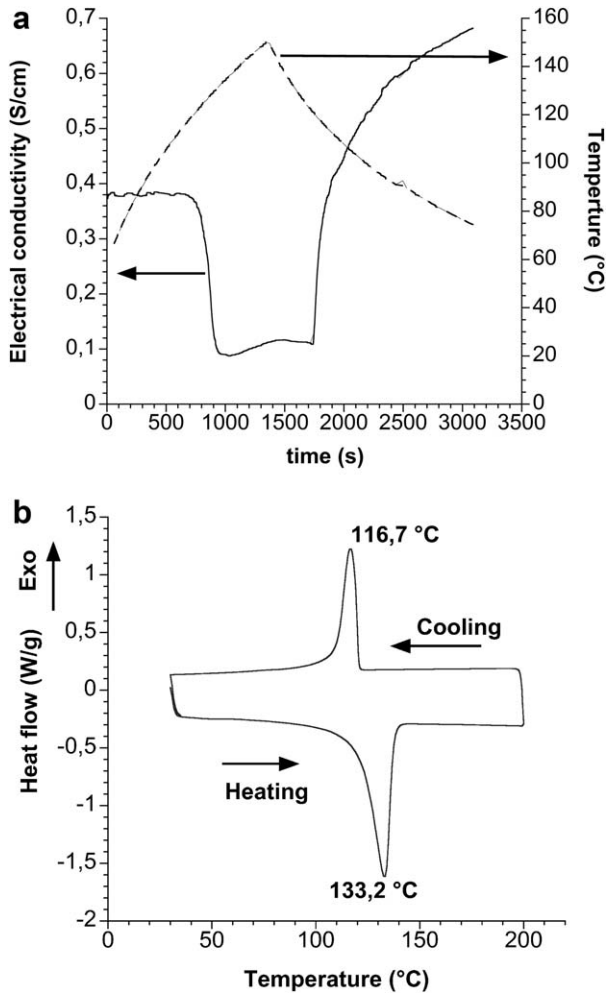

Figure 10. (a) The temperature dependence of conductivity for the bi-component fibers during annealing and (b) DSC curve for the 26 vol % CB/HDPE composite during heating and cooling.

conductivity of the fibers versus the godet (bottom and middle rolls) temperature.

The additional thermal energy supplied by the godet rolls during the cold drawing stage increased the polymer chain mobility in the core matrix and thus enhanced the rearrangement and restoration of the CB network. Figure 9 shows that the conductivity was affected already at temperatures well below T_m of the core; around 70°C a gradual increase was initiated. It is likely that the core material starts to soften with an associated increased molecular mobility at these temperatures as indicated by the broad melting peak in Figure 10(b). Around 100°C the melting become more pronounced, accompanied by a thermal expansion and the increase in conductivity is flattening out. The surrounding PA6 sheath is still solid and withstanding the spin line forces giving the molecular reorientation required for achieving desired mechanical properties of the spun fibers.

However, the fiber conductivity is not restored to the values of the undrawn strands, see Figure 2. This is probably due to a reduction in contact points between the filler particles due to a break up of CB clusters during the melt extension. It can be argued that the short residence time on the rolls does not allow for a complete recovery of the CB network. To study the influence of the heating time on the conductivity, a yarn was placed in an oven, slightly tensed and clamped to avoid shrinkage during heat treatment. The electrical conductivity remained however the same as that of fibers annealed on the godet rolls although the treatment time was extended. An extension of the heat treatment time thus had no influence on the fiber conductivity. As seen in Figure 10(a), the fibers were heated and the

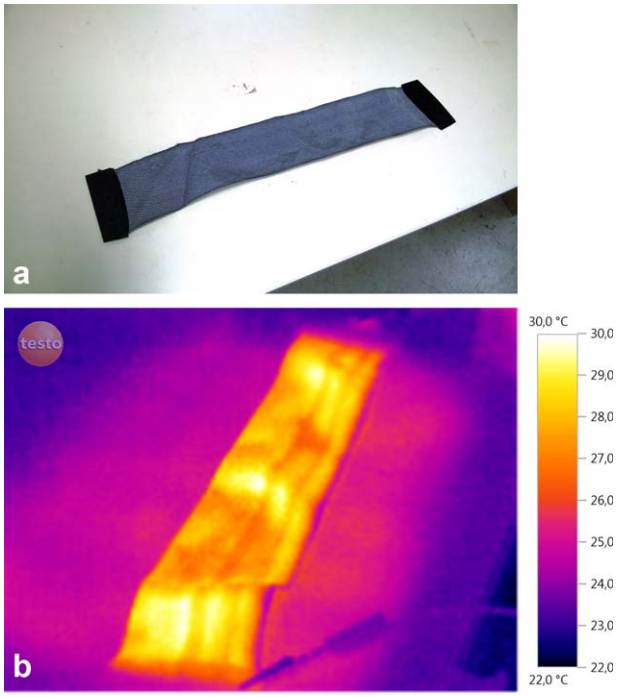

Figure 11. (a) A woven band with the conducitve bi-compoent fibers in the warp direction and (b) corsponding IR image when 48 V was applied. [Color figure can be viewed in the online issue, which is available at wileyonlinelibrary.com.]

core composite started to melt, leading to a decrease in conductivity due to a breakage of the CB network as a result of thermal expansion and melting of the crystalline HDPE matrix.[30,31] Figure 10(b) Shows DSC thermograms from the first heating and subsequent cooling of pelletized core material, confirming that the melting and re-crystallization agrees well with the decrease and increase in conductivity observed during heating and cooling of the fibers in the oven, Figure 10(a).

From the fibers a weave was formed in an industrial band weaving machine with the conductive fibers in warp direction, see Figure 11(a). The heating ability of the fabric was demonstrated by applying 48–84 V DC to a 40 cm long sample, see Figure 11(b). The surface temperature of the fabric increased from 20°C to 30°C when 48V was applied as seen from the image taken by an IR camera. When the voltage was gradually raised up to 84V a temperature increase up to 35°C was noted.

CONCLUSIONS

Experimental results from spinnability trials show that a low-structured CB/HDPE composite exhibited a spinnability that was superior to that of a high-structured CB/HDPE composite due to structural differences in the CB network in the two composite fibers. The rheological studies pointed to that a higher yield stress was associated with a poorer spinnability.

The low-structured CB/HDPE was incorporated into the core of a bi-component fiber suitable for heating applications. Increasing the solid state drawing temperature and in line annealing above the melting point of the conductive core enhanced the mobility of the polymer molecules and thus restored the conductive pathways in the CB network without influencing the mechanical properties of the fibers. The resulting conductivity of the fibers was shown to be independent of the annealing time. The recovery of the CB network due to the heat treatment took place in less than 1 second. Thus it is possible to produce melt spun textile fibers with a conductivity of 1.5 S/cm. The fibers are suitable for car seat heating or in similar applications where high voltages energy supplies are available.

ACKNOWLEDGMENTS

The authors thank SSF (Swedish Foundation for Strategic Research) and Vinnova (The Swedish Governmental Agency for Innovation Systems) for financial support.

REFERENCES

1. Schoeser, M. World Textiles: A Concise History; Thames & Hudson: London, **2003**.
2. Mattila, H. Intelligent Textiles and Clothing; Burlington: Woodhead Publishing, **2006**.
3. Jiang, S. Q.; Guo, R. H. Modification of Textile Surfaces Using Electroless Deposition, In Surface Modification of Textiles; Wei, Q., Ed.; Woodhead Publishing: Cambridge, UK, **2009**, pp 108–125.
4. Trumsina, E.; Kukle, S.; Zommere, G. *Rigas Tehniskas Universitates Zinatniskie Raksti.* **2012**, *7*, 107.
5. Strååt, M.; Boldizar, A.; Rigdahl, M.; Hagström, B. *Polym. Eng. Sci.* **2011**, *51*, 1165.
6. Strååt, M.; Toll, S.; Boldizar, A.; Rigdahl, M.; Hagström, B. *J. Appl. Polym. Sci.* **2011**, *119*, 3264.
7. Strååt, M.; Rigdahl, M.; Hagström, B. *J. Appl. Polym. Sci.* **2012**, *123*, 936.
8. Nilsson, E.; Oxfall, H.; Wandelt, W.; Rychwalski, R.; Hagström, B. *J. Appl. Polym. Sci.* **2013**, *130*, 2579.
9. Li, B.; Zhong, W.-H. *J. Mater. Sci.* **2011**, *46*, 5595.
10. Lau, K.-T.; Gu, C.; Hui, D. *Compos. Part B: Eng.* **2006**, *37*, 425.
11. Kim, H.; Abdala, A. A.; Macosko, C. W. *Macromolecules* **2010**, *43*, 6515.
12. Dondero, W. E.; Gorga, R. E. *J. Polym. Sci. Part B: Polym. Phys.* **2006**, *44*, 864.
13. Haggenmueller, R.; Gommans, H. H.; Rinzler, A. G.; Fischer, J. E.; Winey, K. I. *Chem. Phys. Lett.* **2000**, *330*, 219.
14. Pötschke, P.; Kobashi, K.; Villmow, T.; Andres, T.; Paiva, M. C.; Covas, J. A. *Compos. Sci. Technol.* **2011**, *71*, 1451.
15. Laun, H. M.; Schuch, H. *J. Rheol.* **1989**, *33*, 119.
16. Balberg, I. *Phys. Rev. Lett.* **1987**, *59*, 1305.
17. Rahaman, M.; Chaki, T. K.; Khastgir, D. *J. Mater. Sci.* **2011**, *46*, 3989.
18. Gkourmpis, T. *Carbon-Based High Aspect Ratio Poymer Nanocomposites*, In Nanoscience and Computational Chemistry; Apple Academic Press, **2013**, p 85.
19. Mallette, J. G.; Quej, L. M.; Marquez, A.; Manero, O. *J. Appl. Polym. Sci.* **2001**, *81*, 562.
20. Ren, D.; Zheng, S.; Wu, F.; Yang, W.; Liu, Z.; Yang, M. *J. Appl. Polym. Sci.* **2014**, 131.
21. Weber, M.; Kamal, M. R. *Polym. Compos.* **1997**, *18*, 711.
22. Chen, X. L.; Cui, P.; Ji, Y. P. *Appl. Mech. Mater.* **2013**, *333–335*, 1872.
23. Yui, H.; Wu, G.; Sano, H.; Sumita, M.; Kino, K. *Polymer* **2006**, *47*, 3599.
24. Carbon Black, In Kirk-Othmer Encyclopedia of Chemical Technology; John Wiley & Sons, Inc: Hoboken, NJ, **2007**, p 761.
25. Ziabicki, A. Fundamentals of Fibre Formation, 1st ed.; Wiley: Bath, **1976**.
26. Nakajima, N.; Bowerman, H. H.; Collins, E. A. *J. Appl. Polym. Sci.* **1977**, *21*, 3063.
27. White, J. L.; Czarnecki, L.; Tanaka, H. *Rubber Chem. Technol.* **1980**, *53*, 823.
28. White, J. L.; Tanaka, H. *J. Appl. Polym. Sci.* **1981**, *26*, 579.
29. Tanaka, H.; White, J. L. *Polym. Eng. Sci.* **1980**, *20*, 949.
30. Meyer, J. *Polym. Eng. Sci.* **1973**, *13*, 462.
31. Lee, G. J.; Kyung Do, S.; Im, S. S. *Polym. Eng. Sci.* **1998**, *38*, 471.